

# Journal of Advanced Research in Applied Sciences and Engineering Technology

Journal homepage: https://semarakilmu.com.my/journals/index.php/applied\_sciences\_eng\_tech/index ISSN: 2462-1943



# Inverse C-shaped Complementary Split-ring Resonator-based NRI Metaatom for Wireless Applications

Mohammad Jakir Hossain<sup>1,\*</sup>, Md. Jakirul Islam<sup>1</sup>, Momotaz Begum<sup>1</sup>, Md. Reazul Hoque<sup>2</sup>, Khan Md. Foysol<sup>3</sup>, Mehedi Hasan Tohin<sup>1</sup>, Sikder Sunbeam Islam<sup>4</sup>, Mohammad Rashed Iqbal Faruque<sup>5</sup>, Sabirin Abdullah<sup>5</sup>\*

- <sup>1</sup> Department of Electrical and Electronic Engineering, Dhaka University of Engineering & Technology, Gazipur, Bangladesh
- <sup>2</sup> Department of Electrical and Electronic Engineering, Ahsanullah University of Science and Technology, Dhaka, Bangladesh
- Electrical and Electronic Engineering, Textile Engineering College, Noakhali (TECN), Bangladesh
- Department of Electrical and Electronic Engineering. International Islamic University Chittagong, Chittagong, Bangladesh
- <sup>5</sup> Space Science Centre (ANGKASA), Universiti Kebangsaan Malaysia, 43600 UKM, Bangi, Selangor, Malaysia

#### **ARTICLE INFO**

#### **ABSTRACT**

This study investigates a meta-atom exhibiting a broad Negative Refractive Index (NRI). The meta-atom is constructed using a complementary circular-square split-ring resonator shaped in an inverse C design. The electromagnetic properties of the structure were analyzed through simulations using CST Microwave Studio, Ansys HFSS 3D software, and ADS. The meta-atom demonstrates three distinct resonant frequencies at 2.71 GHz, 4.19 GHz, and 5.60 GHz, spanning both the S- and C-bands. Its optimal Effective Medium Ratio (EMR) is 12.30, and the unit cell measures 9 mm × 9 mm with a substrate thickness of 0.508 mm. This design is notable for its compact dimensions, strong NRI performance, high EMR, and well-defined resonance points. The S-band, commonly used for radar, and the C-band, which supports high-speed Wi-Fi networks, are both covered by this structure. The paper outlines the design methodology and various parameter optimization processes. Simulation results from Ansys HFSS align well with those from CST and ADS. Additionally, the study includes an analysis of surface current distributions, as well as the electric (E-field) and magnetic (Hfield) field patterns. Compared to alternative designs discussed in the article, this proposed structure offers superior performance, showcasing a high EMR, extensive NRI range, and a compact form factor suitable for radar and Wi-Fi applications.

## Keywords:

Meta-atom; Negative Refractive Index (NRI); Effective Medium Ratio (EMR); Wi-Fi network; wireless communication

#### 1. Introduction

Metamaterials are synthetic materials engineered to exhibit unique properties that are not naturally present in conventional materials. They consist of structured elements known as meta-

\* Corresponding author.

E-mail address: jakir@duet.ac.bd

\* Corresponding author.

E-mail address: dr\_sabirin@ukm.edu.my

https://doi.org/10.37934/araset.64.4.158172

atoms, which are arranged periodically and interact with electromagnetic waves in unconventional ways. This enables unprecedented control over these waves.

The idea of metamaterials arose from the desire to manipulate electromagnetic waves and light at a microscopic level, which has led to innovative advancements in various scientific and technological domains [1]. The concept was first proposed by Sir John Pendry in the 1990s, who introduced the possibility of materials with a Negative Refractive Index (NRI), challenging the longheld belief that refractive indices must always be positive. Pendry demonstrated that by designing specific geometric structures with particular electromagnetic properties, it is possible to create materials with a Negative Refractive Index, resulting in phenomena such as negative refraction and subwavelength imaging [2]. Negative refraction leads to the reversal of the propagation of electromagnetic waves, enabling imaging below the diffraction limit, a phenomenon known as subwavelength imaging. In contrast to traditional materials, which are often curved, this behavior allows light to propagate across an electromagnetically flat surface. A Negative Refractive Index is also characterized by an antiparallel phase velocity [3]. These distinctive and counterintuitive features have found practical applications in controlling electromagnetic waves, particularly in wireless and communication systems. As a result, the study and development of metamaterials have attracted significant attention across diverse fields like optics, electromagnetics, acoustics, and materials science. Researchers and engineers have developed various methods to design and fabricate metamaterials with specific desired traits such as NRI, electromagnetic cloaking, perfect absorption, and chiral response [4]. For instance, Shahidul et al., in [5] introduced an Epsilon-Negative (ENG) metamaterial using a crossed-line complementary split-ring resonator (CSRR), with an EMR of 4.5 and a unit cell size of 10 mm × 10 mm. Hossain et al., proposed a meta-atom with an EMR of 10.55, designed for multiband applications, with a unit cell size of 12 mm × 12 mm × 1.6 mm [6]. Hasan et al., presented a double-negative (DNG) Z-shaped metamaterial, which claimed a broad Xband range and a low EMR of 4 [7]. A Negative Refractive Index metamaterial for C- and X-band applications was reported by Hossain et al.,

The design structure has a size of 10 mm by 10 mm by 1.6 mm. EMR of 9.55 [8] has been attained. A modified hexagonal epsilon-negative metamaterial tri-band wireless application was proposed by Afsar et al., The modified hexagonal split ring resonator that makes up the given metamaterial unit cell form has an EMR of 11.53 and a design structure is 9 mm × 9 mm × 1.6 mm [9]. A "double T-Ushaped" biaxial compact DNG metamaterial unit-cell with dimensions of 10.5 × 11 × 1.6 mm<sup>3</sup> and an EMR of 14.28 along the z-axis was proposed by Hossain et al., for multiband applications [10]. Zhou et al., published a 12 × 12 mm<sup>2</sup> SNG metamaterial unit cell that was "S-shaped," suitable for the Xand Ku-bands, and had an EMR of less than 4 [11]. A metamaterial sensor was also described by Islam et al., in order to demonstrate the structure's sensitivity. Metamaterial has a meander line structure, and its sensitivity and EMR are, respectively, -3 dB/mm and 7.2 [12]. Almutairi et al., demonstrated a DNG metamaterial that has an EMR of 7.44, a size of 5.5 × 5.5 mm<sup>2</sup>, and is solely suitable in the Cband [13]. For dual-band microwave applications, Farugue et al., created a DNG metamaterial; nevertheless, the unit cell structure is relatively large size of 25 × 20 mm<sup>2</sup> [14]. A hexagonal SRRbased metamaterial for S- and X-band applications was first introduced by Islam et al., Its dimensions are 10 × 10 mm<sup>2</sup>, and its EMR is 8.40 [15]. Hossain et al., presented a metamaterial for a left-handed multiband meta-atom that obeys EMR, however it is only 11 × 10 mm<sup>2</sup> in size [16]. The challenges or limitations in existing metamaterials are low EMR value and attaining the broader NRI value for Wi-Fi and radar applications.

Other notable contributions include a Negative Refractive Index metamaterial for C- and X-band frequencies, a modified hexagonal epsilon-negative structure for tri-band wireless applications, and a biaxial compact DNG unit-cell designed by Hossain *et al.*, for multiband uses. Despite the progress,

current metamaterial designs still face challenges such as low EMR values and limited NRI ranges for applications in Wi-Fi and radar systems. This study introduces a new NRI meta-atom design, incorporating a complementary circular-square split-ring resonator based on an inverted C-shape.

The proposed meta-atom features three resonance frequencies: 2.71 GHz, 4.19 GHz, and 5.60 GHz, which span the S-band (2–4 GHz) and C-band (4–8 GHz), used for applications like radar communication, Wi-Fi, satellite telemetry, and air traffic management. The NRI regions of the meta-atom, where it exhibits a Negative Refractive Index, were observed between 2.16–2.51 GHz, 2.96–4.17 GHz, and 4.21–7.48 GHz. The study also explores the surface current, electric and magnetic fields, and the effective medium properties of the structure, concluding that the inverted C-shaped NRI meta-atom offers an optimal solution with an EMR of 12.30, combining compactness and efficiency for radar and Wi-Fi applications.

# 2. Methods and Techniques

# 2.1 Design of the Meta-Atom Unit Cell

Split-ring resonators (SRRs) are widely used components in the creation of metamaterials. Originally, these resonators were developed from materials typically used in circuit boards. A periodic arrangement of SRRs was first employed to demonstrate the concept of a negative refractive index (NRI) [17]. As a result, this research utilizes NRI meta-atoms that are based on complementary circular-square split-ring resonators. The design of the proposed two-layer meta-atom, as shown in Figure 1, comprises both a metal layer and a dielectric layer. The resonator structures are made of copper and have an inverse C-shaped complementary split-ring design. The dielectric material used is Rogers RO4003C, with the substrate dimensions measuring 9 mm × 9 mm and a thickness of 0.508 mm. The substrate has a dielectric constant ( $\epsilon$ ) of 3.55 and a loss tangent ( $\delta$ ) of 0.0027. This metaatom features a combination of two circular and three-square split-ring resonators, all complementing each other. Embedded inside these resonators is an inverted C-shaped structure. The copper resonators are 0.035 mm thick, with a conductivity ( $\sigma$ ) of 5.8  $\times$  10<sup>7</sup> S/m. The circular resonators have a gap width of 0.3 mm, while the square resonators and the inverted C-shape have a gap of 0.6 mm. The spacing between the circular rings is 0.2 mm, with all rings, except for the inverse C-ring, having widths of 0.4 mm. The inverse C-ring has a width of 0.6 mm, and the recommended gaps for the circular and square rings are 0.25 mm and 0.30 mm, respectively. Figure 2 illustrates the proposed resonator on the Rogers RO4003C substrate.

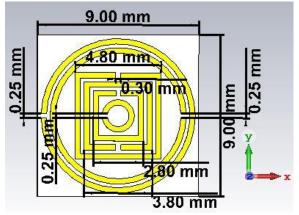
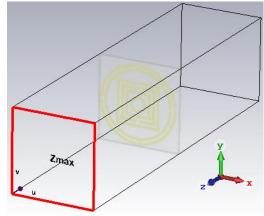


Fig. 1. Front view with dimension of the unit cell



**Fig. 2.** Perspective view with ports of the unit cell

The outer boundary form of the suggested meta-atom unit cell is shown in Figure 2. To simulate the meta-atom, the finite element method was employed using CST Microwave Studio software (2019 version).

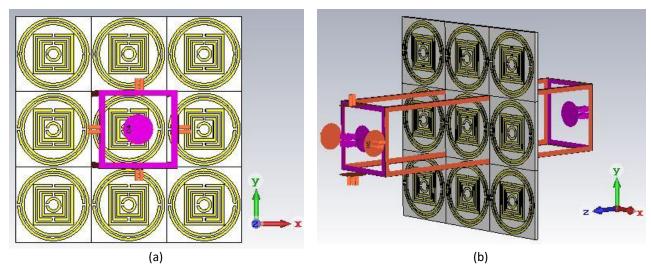


Fig. 3. (a) Front view of the array of the unit cell (b) Boundary setup of the proposed structure

Boundary conditions were applied in the x and y directions, while electromagnetic waves were applied in the negative z-direction, as shown in Figure 3. Open space conditions at each port were included to facilitate the analysis of resonance frequencies and their field properties, as seen in Figure 4. A frequency-domain solver was used to simulate the inverse C-shaped cell in the frequency range from 0.5 GHz to 8 GHz. The S-parameters (S11 and S21) were determined from the unit cell simulations over the specified frequency range. The Nicolson-Ross-Weir (NRW) method, a widely recognized approach for electromagnetic characterization, was used to calculate the effective medium parameters such as refractive index  $(\eta)$ , relative permittivity  $(\varepsilon)$ , and permeability  $(\mu)$  from the simulated scattering parameters. In the NRW method, composite terms V1 and V2 are used to add and subtract scattering characteristics to calculate these effective medium parameters [18,19].

Here, the following Eq. (1), Eq. (2), Eq. (3), Eq. (4) are used to derive the characteristics such as  $\varepsilon_r$ ,  $\mu_r$ ,  $\eta$ , and Z of the meta-atoms.

$$\varepsilon_r = \frac{2}{jk_0d} \frac{1 + S_{11} - S_{21}}{1 - S_{11} + S_{21}} \tag{1}$$

$$\mu_r = \frac{j2S_{11}}{jk_0d} + \mu_0 \tag{2}$$

$$\eta = \frac{2}{jk_0 d} \sqrt{\frac{(S_{21} - 1)^2 - S^2_{11}}{((S_{21} + 1)^2 - S^2_{11}}}$$
(3)

$$Z = \sqrt{\frac{\mu_r}{\varepsilon_r}} \tag{4}$$

The wave number in this instance is  $k_0$ , while the substrate's thickness is d.

#### 2.2 Design Process of the Proposed Meta-Atom Unit Cell

The design of the proposed NRI meta-atom unit cell, based on an inverse C-shaped complementary split-ring resonator, involves a combination of three circular and three-square split-ring resonators. This configuration is an adaptation of the traditional SRR. To enhance the capacitive and inductive effects, four additional SRRs are positioned within the outer two rings. The overall design uses a PEC (perfect electric conductor) mounted on a cost-effective Rogers RO4003C substrate. Initially, two designs, Design 1 and Design 2, are created and analyzed. The results from these initial designs are then used to develop Design 3 by merging the features of the first two designs for better performance. Following this, Design 4 through Design 6 is developed to achieve higher efficiency. The final design incorporates an inverted C-shaped ring within the square rings, resulting in the optimal configuration, as depicted in Figure 4. The analysis of these designs is shown in Figure 5 (a) and (b).

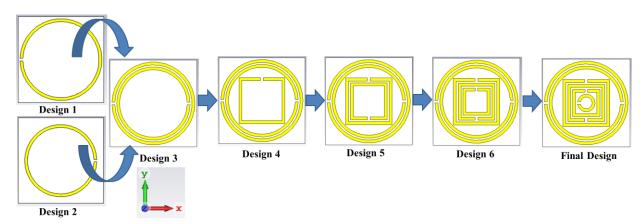
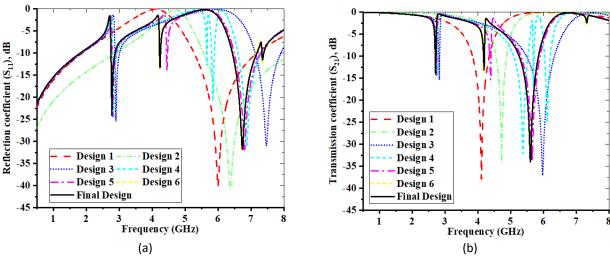


Fig. 4. Various structural configurations used to select the final unit cell structure

Figure 5 (a) and (b) presents the reflection (S11) and transmission (S21) coefficients for the different design configurations. Design 1 features a circular split-ring resonator, which exhibits a resonance frequency with S11 at -40.181 dB at 5.999 GHz and S21 at -38.289 dB at 4.109 GHz, covering the C-band. Design 2 also demonstrates a resonance within the C-band, with S11 at -40.724 dB at 6.365 GHz and S21 at -34.891 dB at 4.723 GHz. Design 3 exhibits S11 magnitudes of -26.592 dB and -30.878 dB at 2.900 GHz and 7.469 GHz, respectively, and S21 magnitudes of -16.412 dB and -37.286 dB at 2.825 GHz and 5.975 GHz, respectively, spanning both the S- and C-bands. Design 4 displays S11 magnitudes of -25.233 dB, -20.997 dB, and -30.798 dB at 2.833 GHz, 5.845 GHz, and 6.877 GHz, and S21 at -14.543 dB, -32.322 dB, -18.048 dB, and -25.455 dB at 2.763 GHz, 5.374 GHz, 5.697 GHz, and 6.118 GHz, covering both the S- and C-bands. Design 5 shows S21 magnitudes of -15.434 dB, -15.878 dB, and -34.199 dB at 2.734 GHz, 4.393 GHz, and 5.653 GHz, with S11 magnitudes of -23.818 dB, -14.494 dB, and -31.907 dB at 2.794 GHz, 4.445 GHz, and 6.803 GHz. The final design shows S11 magnitudes of -25.160 dB, -13.643 dB, and -31.51 dB at 2.710 GHz, 4.175 GHz, and 5.60 GHz, and S21 magnitudes of -14.162 dB, -13.875 dB, and -33.447 dB at 2.86 GHz, 5 GHz, and 8 GHz, respectively. This final design achieves the desired resonance frequencies and a higher EMR, making it superior to the earlier configurations.



**Fig. 5.** Frequency vs. scattering parameters (a) Reflection coefficient (S11), (b) Transmission coefficient (S21) of the proposed structure

#### 3. Result and Discussion

# 3.1 Scattering Parameters and Meta-Atom Properties

Figure 6 presents the S-parameters for the proposed unit cell, which exhibits three distinct resonance frequencies for both reflection and transmission. For the transmission coefficient (S21), the resonance frequencies occur at 2.328 GHz, 4.190 GHz, and 5.600 GHz, with corresponding magnitudes of -14.930 dB, -13.579 dB, and -34.113 dB. The -10 dB bandwidths for S21 are between 2.71 and 2.72 GHz, 4.18 and 4.20 GHz, and 5.26 and 5.85 GHz in the CST simulator. In the HFSS simulator, S21 shows resonance frequencies at 2.714 GHz, 4.262 GHz, and 5.706 GHz, with magnitudes of -13.813 dB, -13.228 dB, and -33.025 dB, and the -10 dB bandwidths are from 2.71 to 2.72 GHz, 4.25 to 4.27 GHz, and 5.40 to 5.92 GHz. The ADS simulator results show S21 resonances at 2.712 GHz, 4.256 GHz, and 5.512 GHz, with magnitudes of -49.021 dB, -45.153 dB, and -62.387 dB. The -10 dB bandwidths range from 2.33 to 2.85 GHz, 3.86 to 4.33 GHz, and 4.66 to 6.32 GHz.

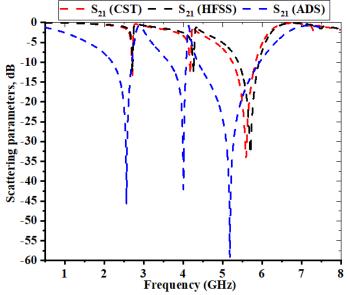


**Fig. 6.** Frequency versus scattering parameters in dB by three softwares

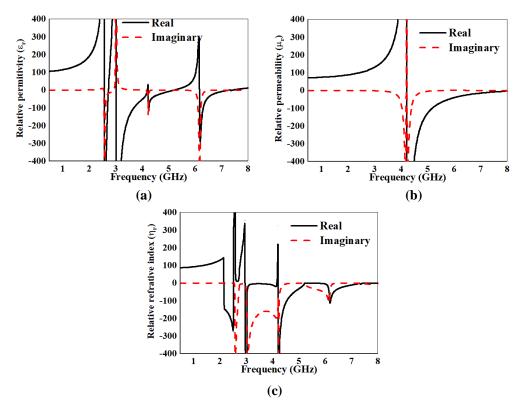


**Fig. 7.** Frequency versus (a) Relative permittivity ( $\epsilon$ ) (b) Relative permeability ( $\mu$ ), (c) Relative reflective index ( $\eta$ )

Using the NRW method outlined in Eq. (1), Eq. (2), Eq. (3), Eq. (4), the effective medium parameters such as the relative permittivity ( $\epsilon_r$ ), relative permeability ( $\mu_r$ ), and refractive index ( $\eta$ ) were derived from the scattering parameters. MATLAB software was used to calculate these parameters, and their real and imaginary components are shown in Figures 7 (a), (b), and (c). The Negative Refractive Index of the proposed meta-atom unit cell is clearly evident. The NRI frequency range is observed between 2.16 to 2.51 GHz, 2.96 to 4.17 GHz, and 4.21 to 7.48 GHz in the CST simulation. Results from CST, HFSS, and ADS simulators were compared in Figure 12, demonstrating consistent reflection and transmission coefficients across all simulators.

#### 3.2 Parametric Analysis

This section examines the factors affecting the performance of the meta-atom, including the choice of substrate material, the impact of different conducting materials on scattering parameters, variations in the structural dimensions, adjustments to the split gaps in the conducting material, and the effects of substrate thickness. The subsequent section will address the analysis of surface current, electric field, and magnetic field distributions.

#### 3.2.1 Impact of substrate material

Various substrate materials were tested, including Rogers RO4350B (lossy), RO4003C (lossy), and FR-4 (lossy), each with different dielectric constants, electric loss tangents, and thicknesses. For instance, Rogers RO4350B has a dielectric constant of 3.66, a loss tangent of 0.0037, and a thickness of 0.508 mm.

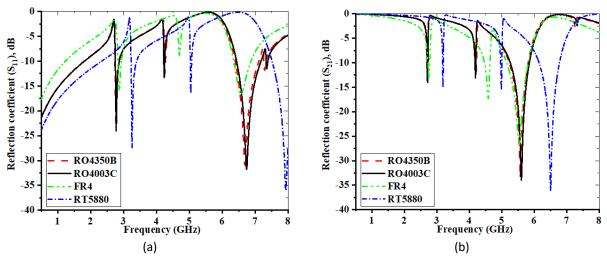


**Fig. 8.** Frequency versus scattering parameters (a) Reflection coefficient,  $S_{11}$ , (b) Transmission coefficient,  $S_{21}$  for different substrate materials

The S11 magnitudes for this material were -24.218 dB, -12.417 dB, and -31.064 dB at 2.765 GHz, 4.265 GHz, and 6.688 GHz, respectively, and the corresponding S21 values were -13.696 dB, -12.956 dB, and -33.285 dB at 2.705 GHz, 4.213 GHz, and 5.571 GHz, respectively, covering the S- and C-bands. Similar tests were performed on the other materials. Based on these results, Rogers RO4003C was selected for its optimal performance in terms of coverage band, EMR, necessary frequencies, and scattering parameter magnitudes. Figure 8 (a) and (b) displays the S11 and S21 vs. frequency for different substrates. It was found that the permittivity of the material inversely affects the capacitance, which in turn influences the resonance frequency, with lower permittivity leading to higher resonance frequencies.

# 3.2.2 Effect of conducting material split

Figure 9 illustrates the influence of varying the split gap between the conducting patches on the reflection (S11) and transmission (S21) coefficients. Four split gap values of 0.1, 0.25, 0.4, and 0.55 mm were tested. For a gap of 0.1 mm, S11 magnitudes were -25.559 dB, -13.899 dB, and -31.541 dB at 2.773, 4.280, and 6.661 GHz and S21 magnitudes were 14.754 dB, 14.034 dB, and 33.106 dB at 2.712, 4.235, and 5.599 GHz

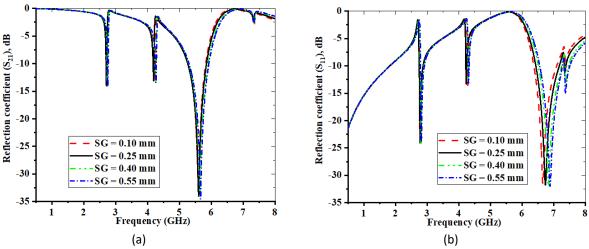


**Fig. 9.** Frequency versus scattering parameters in dB (a) Reflection coefficient,  $S_{11}$ , (b) Transmission coefficient,  $S_{21}$  for different split of patch

For a gap of 0.25 mm, S11 magnitudes were -24.674 dB, -13.373 dB, and -31.65 dB at 2.773, 4.238, and 6.744 GHz, and S21 magnitudes were -14.930 dB, -13.579 dB, and -34.113 dB at 2.712, 4.190, and 5.60 GHz. For a split gap of 0.4 mm, the amplitudes of  $S_{11}$  were - 24.705, - 13.702, and - 31.987 dB at frequencies of 2.811, 4.302, and 6.838 GHz, respectively. The amplitudes of  $S_{21}$  were - 14.754, -13.866, and - 34.585 dB at frequencies of 2.742, 4.258, and 5.645 GHz, respectively. With a split gap of 0.55 mm, the amplitudes of  $S_{11}$  were -24.705, -12.878, and -31.805 dB at frequencies of 2.817 GHz, 4.317 GHz, and 6.893 GHz, respectively. The amplitudes of  $S_{21}$  were -15.222, -13.903, and -34.357 dB at frequencies of 2.758 GHz, 4.265 GHz, and 5.657 GHz, respectively. Increasing the split gap leads to higher resonance frequencies. The optimal performance was achieved with a gap of 0.25 mm, which is recommended for the meta-atom design.

# 3.2.3 Effects of conducting material on scattering parameters

Figure 10 shows how different conducting materials affect the scattering parameters. Several metals, including gold, nickel, copper, and platinum, were used as conductors. The amplitudes of S11 and S21 varied with the conductor material. For example, with gold as the conductor, S11 and S21 reached their highest values at frequencies of 2.795, 4.303, and 6.770 GHz, and 2.735, 4.258, and 5.631 GHz, respectively. For nickel as the conducting patch, the amplitudes of  $S_{11}$  were -9.664 dB, -11.40 dB, and - 6.219 dB at frequencies of 2.537 GHz and 5.132 GHz. The values of  $S_{21}$  were -2.673 dB and -10.031 dB at frequencies of 2.537 GHz and 5.132 GHz, respectively. For copper, the S11 magnitudes were -14.930 dB, -13.579 dB, and -34.113 dB at 2.712, 4.190, and 5.60 GHz, while S21 was -14.930 dB, -13.579 dB, and -34.113 dB at the same frequencies. For the conducting patch of FR4, the amplitudes of  $S_{11}$  and  $S_{21}$  were -20.555, -10.140, and -27.057 dB at frequencies of 2.792, 4.296, and 6.761 GHz, and -10.732, -10.252, and -28.373 dB at frequencies of 2.724, 4.243, and 5.604 GHz, respectively. Based on the comparison, copper was chosen as the optimal conducting material due to its favorable scattering parameter performance.

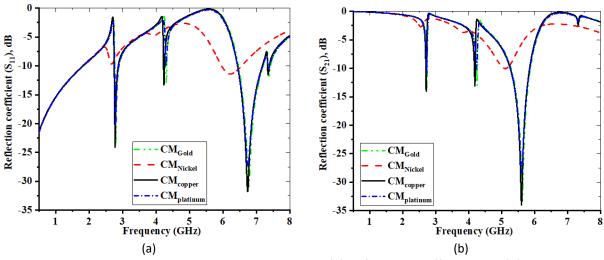


**Fig. 10.** Frequency versus scattering parameters in dB (a) Reflection coefficient,  $S_{11}$ , (b) Transmission coefficient,  $S_{21}$  for different conducting materials

#### 3.2.4 Effect of structural dimensions

Figure 11 presents the S21 response for various meta-atom sizes:  $9 \times 9$  mm<sup>2</sup>,  $10 \times 10$  mm<sup>2</sup>,  $11 \times 11$  mm<sup>2</sup>, and  $12 \times 12$  mm<sup>2</sup>.

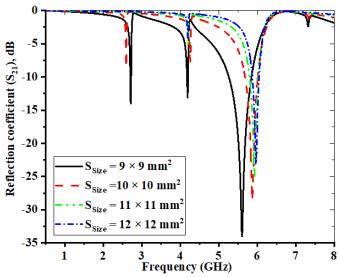
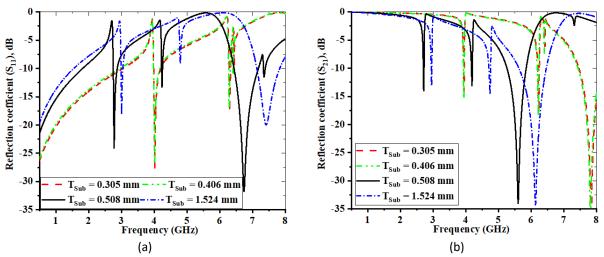


**Fig. 11.** Frequency versus transmission coefficient in dB for different structure size

The 9  $\times$  9 mm² unit cell displayed resonance frequencies at 3.90 and 6.79 GHz with S21 values of -26.35 dB and -31.31 dB, respectively, covering both the S- and C-bands with an EMR of 12.30. For a unit cell size of  $10 \times 10$  mm², the S<sub>21</sub> had a resonance frequency of 5.87 GHz with a magnitude of -28.76 dB, covering only the C-band with an EMR of 5.11. For a unit cell size of  $11 \times 11$  mm2, the S<sub>21</sub> had a magnitude of -25.47 dB at a resonance frequency of 5.92 GHz, covering only the C-band with an EMR of 4.61. For a unit cell size of  $12 \times 12$  mm², the S<sub>21</sub> had a magnitude of -23.23 dB at a resonance frequency of 5.97 GHz, covering only the C-band with an EMR of 4.19. For larger sizes, the resonance frequencies shifted and the EMR decreased. The  $9 \times 9$  mm² size was found to provide the highest EMR and the most favorable resonance frequencies, making it the preferred choice for radar and Wi-Fi applications.

#### 3.2.5 Influence of substrate thickness

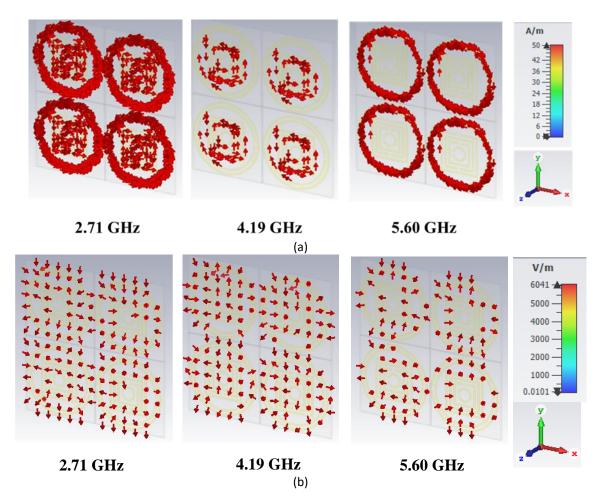
The effect of varying substrate thickness on the scattering parameters was evaluated for thicknesses of 0.305 mm, 0.406 mm, 0.508 mm, and 1.524 mm. At a thickness of 0.305 mm,  $S_{11}$  and  $S_{21}$  have amplitudes of - 28.933 dB and - 17.764 dB at 4.018 GHz and 6.302 GHz, respectively, and -15.717 dB, - 18.234 dB, and - 37.180 dB at 3.943 GHz, 6.235 GHz, and 7.843 GHz. For a thickness of 0.406 mm, the magnitudes of  $S_{11}$  and  $S_{21}$  are -27.940 dB, -17.143 dB, and -13.501 dB at 4.009 GHz, 6.287 GHz, and 6.410 GHz, and -15.890 dB, - 18.950 dB, and -36.922 dB at 3.939 GHz, 6.223 GHz, and 7.821 GHz. At a thickness of 0.508 mm, the amplitudes of  $S_{11}$  are -24.674 dB, -13.373 dB, and -31.65 dB at 2.773 GHz, 4.238 GHz, and 6.744 GHz, and the values of  $S_{21}$  are -14.930 dB, -13.579 dB, and -34.113 dB at 2.712 GHz, 4.190 GHz, and 5.60 GHz. When the substrate thickness is 1.524 mm, the magnitudes of  $S_{11}$  and  $S_{21}$  are - 13.335 dB, - 14.652 dB, and - 33.724 dB at 3.006 GHz, 4.790 GHz, and 7.423 GHz, and -13.335 dB, -14.652 dB, and 33.724 dB at 2.955 GHz, 4.744 GHz, and 6.143 GHz. As shown in Figure 12, increasing the substrate thickness resulted in a decrease in resonance frequencies. The 0.508 mm thickness provided the best performance, offering the desired resonance frequencies and magnitudes compared to the other thicknesses, and was selected for the final design.



**Fig. 12.** Frequency versus scattering parameters in dB (a) Reflection coefficient,  $S_{11}$ , (b) Transmission coefficient,  $S_{21}$  for different substrate's thickness

# 3.2.6 Analysis of surface current, electric field, and magnetic field distributions

Different transmission resonance frequencies are used to characterize the surface current of the suggested meta-atom unit cell.



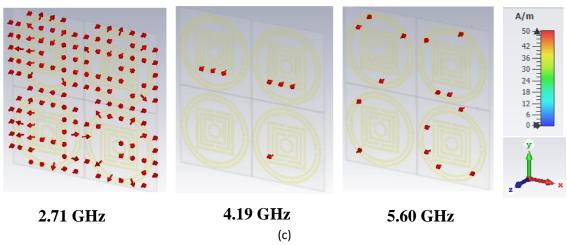


**Fig. 13.** Analysis of EM wave interaction (a) Surface current, (b) Electric field (c) Magnetic field distribution for proposed structure

The surface current distribution for the meta-atom unit cell at the resonance frequencies of 2.71 GHz, 4.19 GHz, and 5.60 GHz is shown in Figure 13 (a). The current intensity varies across different rings, with the strongest intensity in the top circular rings at 2.71 GHz and the outer circular ring at 5.60 GHz. At the first resonance frequency of 2.71 GHz, the current intensity is strong for the top two circular rings and low for the inner square rings. At 4.19 GHz, the surface current intensity is equally spread throughout each square metal ring. At 5.60 GHz, the outer circular ring experiences the strongest intensity of current, while the C-ring and inner ring have the weakest intensity. The E-field and H-field distributions are obtained for various frequencies using CST simulation. The electric field distribution, shown in Figure 13 (b), is nearly uniform across the rings at 2.71 GHz and 4.19 GHz, but more concentrated in the outer ring at 5.60 GHz. At 2.71 GHz and 4.19 GHz, the E-field is nearly equally distributed around the different rings. At 5.60 GHz, the E-field is more concentrated in the outer ring and less concentrated in the middle and inner rings. The resonator rings create a capacitor that stores electrical charge and generates multiple E-fields. The magnetic field distribution, shown in Figure 13 (c), exhibits the expected dipole-like behavior, consistent with the artificial magnetic dipole moment created in the split-ring resonators at each resonance frequency. In a split ring resonator, an artificial magnetic dipole moment is formed when a transverse EM wave travels through a meta-atom. The H-field behavior is demonstrated for the resonance frequencies of 2.71 GHz, 4.19 GHz, and 5.60 GHz.

**Table 1**Comparison between recommended and existing work based on specific factors

[ref]	Unit Cell's Shape	Type of Metamaterial	Size(mm2)	Frequency Bands	EMR	Published Year
[20]	Double C	NRI	12 × 12	S-, C-, X-	7.44	2017
[21]	S-Shaped	SNG	10 × 10	X-	2.4	2017
[22]	Modified H	NRI	$9 \times 9$	X-, Ku-	3.0	2018
[23]	U-joint double split O	NRI	15×12	X-, Ku-	4.5	2019
[24]	Resistor Loaded Sector	SNG	12.5×12.5	S-, C-, X-	NR	2019
[25]	Circular CSRR Shaped	SNG	9×9	S-, C-, X-	9.52	2020
[26]	Concentric Crossed Line	SNG	10×10	C-, X-, Ku	4.5	2020

[27]	Hexagonal	NRI	10×10	S-, X-	8.5	2020
Proposed	Inverse C- shaped	NRI	9×9	S-, C-	12.30	2023

Table 3 provides a comparison between the proposed meta-atom unit cell and existing designs. The proposed structure demonstrates dual-band operation with Negative Refractive Index (NRI) features. According to studies referenced in sources 20, 21, 23, 24, 26, and 27, it is apparent that the unit cell sizes in these designs are larger, with broader frequency coverage but lower Effective Medium Ratio (EMR) compared to the suggested inverse C-shaped meta-atom. Additionally, references 22 and 25 show that while some structures have similar unit cell sizes, their EMR values are still lower than what is achievable with the proposed design. As a result, the performance of the proposed unit cell outperforms those of the previously published structures, as shown in Table 3.

#### 4. Conclusion

This paper presents a Negative Refractive Index (NRI) meta-atom that has been numerically analyzed for radar and Wi-Fi applications. The designed meta-atom achieves three transmission resonance frequencies:  $2.71~\rm GHz$ ,  $4.19~\rm GHz$ , and  $5.60~\rm GHz$ , which cover the S- and C-bands. The total dimensions of the unit cell are  $9\times9\times0.508~\rm mm^3$ , and it exhibits a high EMR value of 12.30. The NRI range of the proposed meta-atom spans from  $2.16~\rm to~2.51~\rm GHz$ ,  $2.96~\rm to~4.17~\rm GHz$ , and  $4.21~\rm to~7.48~\rm GHz$ . The S-band at  $2.71~\rm GHz$  is used for weather radar, while the  $5~\rm GHz$  C-band is frequently applied in Wi-Fi systems for high-speed, large-bandwidth communication. Initially, Wi-Fi was developed for mobile devices like laptops, but today it is widely used in various consumer electronics such as TVs, DVD players, and digital cameras. A parametric analysis of different geometries (lengths and widths) has been carried out to assess the effective medium properties. The simulation results, validated with two commercial software tools, show similar outcomes, confirming the effectiveness of the proposed design. Based on these findings, the proposed meta-atom unit cell demonstrates superior performance compared to other structures discussed in the literature. Due to its compact size, appropriate resonance frequencies, and high EMR, the proposed meta-atom is highly suitable for radar and Wi-Fi applications.

#### Acknowledgment

The authors acknowledge the Research University Grant, Universiti Kebangsaan Malaysia, Geran Translasi, UKM-TR2022-05.

#### References

- [1] Iyer, Ashwin K., Andrea Alu, and Ariel Epstein. "Metamaterials and metasurfaces—Historical context, recent advances, and future directions." *IEEE Transactions on Antennas and Propagation* 68, no. 3 (2020): 1223-1231. https://doi.org/10.1109/TAP.2020.2969732
- [2] Boardman, Allan. "Pioneers in metamaterials: John pendry and victor veselago." *Journal of optics* 13, no. 2 (2010): 020401. <a href="https://doi.org/10.1088/2040-8978/13/2/020401">https://doi.org/10.1088/2040-8978/13/2/020401</a>
- [3] Veselago, V. G. "The electrodynamics of substances with simultaneously negative values of and." *Usp. fiz. nauk* 92, no. 3 (1967): 517-526. <a href="https://doi.org/10.3367/UFNr.0092.196707d.0517">https://doi.org/10.3367/UFNr.0092.196707d.0517</a>
- [4] Góra, Paulina, and Przemysław Łopato. "Metamaterials' application in sustainable technologies and an introduction to their influence on energy harvesting devices." *Applied Sciences* 13, no. 13 (2023): 7742. <a href="https://doi.org/10.3390/app13137742">https://doi.org/10.3390/app13137742</a>
- [5] Islam, Mohammad Shahidul, Mohammad Tariqul Islam, Norsuzlin Mohd Sahar, Hatem Rmili, Nowshad Amin, and Muhammad EH Chowdhury. "A mutual coupled concentric crossed-Line split ring resonator (CCSRR) based epsilon negative (ENG) metamaterial for Tri-band microwave applications." *Results in Physics* 18 (2020): 103292. https://doi.org/10.1016/j.rinp.2020.103292

- [6] Hossain, M. J., M. R. I. Faruque, M. T. Islam, and S. S. Islam. "An effective medium ratio obeying meta-atom for multiband applications." *Bulletin of the Polish Academy of Sciences. Technical Sciences* 65, no. 2 (2017): 139-147. <a href="https://doi.org/10.1515/bpasts-2017-0017">https://doi.org/10.1515/bpasts-2017-0017</a>
- [7] Hasan, Md Mehedi, Mohammad Rashed Iqbal Faruque, Sikder Sunbeam Islam, and Mohammad Tariqul Islam. "A new compact double-negative miniaturized metamaterial for wideband operation." *Materials* 9, no. 10 (2016): 830. https://doi.org/10.3390/ma9100830
- [8] Sinha, Krishnan, Sikder Sunbeam Islam, and Mohammad Jakir Hossain. "A combined WU-shaped NRI metamaterial for dual band microwave application." *Univ J Electr Electron Eng* 7, no. 2 (2020): 81-87. https://doi.org/10.13189/ujeee.2020.070202
- [9] Afsar, Salah Uddin, Mohammad Rashed Iqbal Faruque, Mohammad Jakir Hossain, Mayeen Uddin Khandaker, Hamid Osman, and Sultan Alamri. "Modified hexagonal split ring resonator based on an epsilon-negative metamaterial for triple-band Satellite Communication." *Micromachines* 12, no. 8 (2021): 878. <a href="https://doi.org/10.3390/mi12080878">https://doi.org/10.3390/mi12080878</a>
- [10] Hossain, Mohammad Jakir, Mohammad RI Faruque, and Mohammad T. Islam. "A new double T-U-shaped biaxial compact double-negative meta-atom for multiband applications." *Microwave and Optical Technology Letters* 59, no. 10 (2017): 2551-2557. https://doi.org/10.1002/mop.30764
- [11] Zhou, Zhimou, and Helin Yang. "Triple-band asymmetric transmission of linear polarization with deformed S-shape bilayer chiral metamaterial." *Applied Physics A* 119 (2015): 115-119. <a href="https://doi.org/10.1007/s00339-015-8983-9">https://doi.org/10.1007/s00339-015-8983-9</a>
- [12] Islam, Mohammad Tariqul, Md Rashedul Islam, Md Tarikul Islam, Ahasanul Hoque, and Md Samsuzzaman. "Linear regression of sensitivity for meander line parasitic resonator based on ENG metamaterial in the application of sensing." *Journal of Materials Research and Technology* 10 (2021): 1103-1121. <a href="https://doi.org/10.1016/j.jmrt.2020.12.092">https://doi.org/10.1016/j.jmrt.2020.12.092</a>
- [13] Almutairi, Ali F., Mohammad Shahidul Islam, Md Samsuzzaman, Md Tarikul Islam, Norbahiah Misran, and Mohammad Tariqul Islam. "A complementary split ring resonator based metamaterial with effective medium ratio for C-band microwave applications." *Results in Physics* 15 (2019): 102675. <a href="https://doi.org/10.1016/j.rinp.2019.102675">https://doi.org/10.1016/j.rinp.2019.102675</a>
- [14] Faruque, Mohammad Rashed Iqbal, Eistiak Ahamed, Md Atiqur Rahman, and Mohammad Tariqul Islam. "Flexible nickel aluminate (NiAl2O4) based dual-band double negative metamaterial for microwave applications." *Results in Physics* 14 (2019): 102524. https://doi.org/10.1016/j.rinp.2019.102524
- [15] Islam, Mohammad Shahidul, Md Samsuzzaman, Gan Kok Beng, Norbahiah Misran, Nowshad Amin, and Mohammad Tariqul Islam. "A gap coupled hexagonal split ring resonator based metamaterial for S-band and X-band microwave applications." *IEEE Access* 8 (2020): 68239-68253. <a href="https://doi.org/10.1109/ACCESS.2020.2985845">https://doi.org/10.1109/ACCESS.2020.2985845</a>
- [16] Hossain, Mohammad Jakir, Mohammad Rashed Iqbal Faruque, and Mohammad Tariqul Islam. "Effective medium ratio obeying wideband left-handed miniaturized meta-atoms for multi-band applications." *Journal of Electronic Materials* 47 (2018): 1859-1870. <a href="https://doi.org/10.1007/s11664-017-5974-y">https://doi.org/10.1007/s11664-017-5974-y</a>
- [17] Shelby, Richard A., David R. Smith, and Seldon Schultz. "Experimental verification of a negative index of refraction." *science* 292, no. 5514 (2001): 77-79. <a href="https://doi.org/10.1126/science.1058847">https://doi.org/10.1126/science.1058847</a>
- [18] Luukkonen, Olli, Stanislav I. Maslovski, and Sergei A. Tretyakov. "A stepwise Nicolson–Ross–Weir-based material parameter extraction method." *IEEE antennas and wireless propagation letters* 10 (2011): 1295-1298. https://doi.org/10.1109/LAWP.2011.2175897
- [19] Rothwell, Edward J., Jonathan L. Frasch, Sean M. Ellison, Premjeet Chahal, and Raoul O. Ouedraogo. "Analysis of the Nicolson-Ross-Weir method for characterizing the electromagnetic properties of engineered materials." *Progress In Electromagnetics Research* 157 (2016): 31-47. <a href="https://doi.org/10.2528/PIER16071706">https://doi.org/10.2528/PIER16071706</a>
- [20] Hossain, Mohammad Jakir, Mohammad Rashed Iqbal Faruque, and Mohammad Tariqul Islam. "Design and analysis of a new composite double negative metamaterial for multi-band communication." *Current Applied Physics* 17, no. 7 (2017): 931-939. <a href="https://doi.org/10.1016/j.cap.2017.04.008">https://doi.org/10.1016/j.cap.2017.04.008</a>
- [21] Kumari, Khusboo, Naveen Mishra, and Raghvendra Kumar Chaudhary. "A n ultra-thin compact polarization insensitive dual band absorber based on metamaterial for X-band applications." *Microwave and Optical Technology Letters* 59, no. 10 (2017): 2664-2669. <a href="https://doi.org/10.1002/mop.30797">https://doi.org/10.1002/mop.30797</a>
- [22] Hossain, Toufiq Md, Mohd Faizal Jamlos, Mohd Aminudin Jamlos, Ping Jack Soh, Md Imtiaz Islam, and Rizwan Khan. "Modified H-shaped DNG metamaterial for multiband microwave application." *Applied Physics A* 124 (2018): 1-7. <a href="https://doi.org/10.1007/s00339-018-1593-6">https://doi.org/10.1007/s00339-018-1593-6</a>
- [23] Hoque, Ahasanul, Mohammad Tariqul Islam, Ali F. Almutairi, Mohammad Rashed Iqbal Faruque, Mandeep Jit Singh, and Md Shabiul Islam. "U-joint Double split O (UDO) shaped with split square metasurface absorber for X and ku band application." *Results in Physics* 15 (2019): 102757. https://doi.org/10.1016/j.rinp.2019.102757
- [24] Kalraiya, Sachin, Raghvendra Kumar Chaudhary, and Mahmoud A. Abdalla. "Design and analysis of polarization independent conformal wideband metamaterial absorber using resistor loaded sector shaped resonators." *Journal of Applied Physics* 125, no. 13 (2019). <a href="https://doi.org/10.1063/1.5085253">https://doi.org/10.1063/1.5085253</a>

- [25] Venkateswara Rao, Manikonda, Boddapati Taraka Phani Madhav, Tirunagari Anilkumar, and Badugu Prudhvinadh. "Circularly polarized flexible antenna on liquid crystal polymer substrate material with metamaterial loading." *Microwave and Optical Technology Letters* 62, no. 2 (2020): 866-874. <a href="https://doi.org/10.1002/mop.32088">https://doi.org/10.1002/mop.32088</a>
- [26] Islam, Mohammad Shahidul, Mohammad Tariqul Islam, Norsuzlin Mohd Sahar, Hatem Rmili, Nowshad Amin, and Muhammad EH Chowdhury. "A mutual coupled concentric crossed-Line split ring resonator (CCSRR) based epsilon negative (ENG) metamaterial for Tri-band microwave applications." *Results in Physics* 18 (2020): 103292. <a href="https://doi.org/10.1016/j.rinp.2020.103292">https://doi.org/10.1016/j.rinp.2020.103292</a>
- [27] Islam, Mohammad Shahidul, Md Samsuzzaman, Gan Kok Beng, Norbahiah Misran, Nowshad Amin, and Mohammad Tariqul Islam. "A gap coupled hexagonal split ring resonator based metamaterial for S-band and X-band microwave applications." *IEEE Access* 8 (2020): 68239-68253. <a href="https://doi.org/10.1109/ACCESS.2020.2985845">https://doi.org/10.1109/ACCESS.2020.2985845</a>